

Calorimetric detection of the conical THz radiation from femtosecond laser filaments in air

Aurélien Houard, Yi Liu and André Mysyrowicz^{a)}

Laboratoire d'Optique Appliquée, ENSTA, Ecole Polytechnique, CNRS UMR 7639, 91761, Palaiseau, France

Bernadette Leriche

Institut d'Astrophysique Spatiale, CNRS UMR 861, Université de Paris-Sud, Bat 121, 91405, Orsay, France

The spectral distribution of the conical terahertz (THz) emission from a femtosecond laser filament in air is measured with a bolometric detector and a set of filters, confirming that the main part of the emission lies between 0.5 and 3 THz. The efficiency of this THz emission is compared with that obtained in air via Four Waves Mixing of femtosecond laser pulses at ω and 2ω in the presence of a plasma. © 2007 American Institute of Physics

Recently, several papers have appeared on the production of THz radiation in air with fs laser¹⁻⁶. Of particular interest is the transition-Cherenkov mechanism responsible for a conical emission in the forward direction, since the moving ionization front responsible for the THz emission can be generated in the vicinity of a remote object, several tens or even hundreds of meters away from the laser³. This bypasses the problem of THz attenuation in air due to the presence of water vapor. According to the theoretical model of V. Tikhonchuk³⁻⁴, the spectral peak should lie in the 0.5-4 THz band. Unfortunately, the detector used in ref 3 could only measure the THz component around 0.1 THz, giving no information at higher frequencies.

In this letter we report on measurements of this THz generation process performed with a bolometer. Together with a set of filters it allows to determine the power spectrum of the THz radiation. As expected, the main part of the emission lies between 0.5 and 3 THz. Furthermore, we have compared the efficiencies of this process with a well known and calibrated technique of THz production in air called Four Wave Mixing (FWM), consisting in optical rectification of the fundamental laser beam (ω) with its second harmonic (2ω) in air in the presence of a plasma⁷.

The experimental setup is shown in Figure 1. The laser used is a commercial Ti:Sa CPA (chirped pulsed amplification) laser chain delivering 50 fs pulse at a wavelength of 800 nm. The maximum available energy per pulse was 15 mJ, but to avoid multifilamentation we only used 3.5 mJ. The laser beam had a Gaussian profile with 10 mm FWHM (full width at half-maximum). The laser pulse was focused by a silica convex lens, with a focal length F between 200 and 2000 mm. An off-axis parabola (focal = 5 cm) with a 5 mm hole on the center collected the THz produced by the plasma formed in a ~ 10 cm long region around the geometrical focus of the lens. The hole was necessary to let the filament pass through, thus preventing the creation of a THz emitting plasma on the mirror M . Several filters (Teflon, polyethylene and diamond powder) were used to block totally the residual infrared light of the laser^{b)}. The total transmission of this permanent set of filters allowed detecting radiation between 0.1 and 2.7 THz (see inset in Figure 1 case A). In addition, three optional filters (B, C and D in Figure 1), whose transmissions had been measured with a THz spectrometer could be added in front of the bolometer. A Z-cut quartz lens inside the 4K Dewar focused the THz beam on a silicon bolometer (see ref. 8 for further description of the detector). The electric signal from the bolometer was amplified, and for each measurement it was averaged over 200 shots.

By changing the focal of the lens one can tune the length of the plasma filament and its electron density⁹⁻¹⁰. We measured the spectrum of the THz produced with 5 different lenses $F = 200, 500, 1000, 1600$ and 2000 mm. Table I shows the estimated length of the filament plasma column corresponding to these focal lengths, the total signal measured with the filter A (in mV), and the ratio of this signal in % measured with the three additional filters B, C and D. The following remarks can be made. First, the total THz signal is seen to increase with the focal length up to $F = 1000$ mm and to decrease afterwards. Second, we note that ~ 50 % of the energy lies in the band 0.5-3 THz. Finally, there is a shift towards shorter wavelengths when the filament length is reduced. These features are well explained by the transition-Cherenkov radiation model, as discussed now.

^{a)} Corresponding author: andre.mysyrowicz@ensta.fr

^{b)} An easy check of any residual IR entering the detector is done by placing a THz absorbing glass plate in front of the dewar. No bolometer signal must be observed in this case.

From the theoretical model developed in ref 3-4 the spectral distribution of the transition-Cherenkov THz is mainly given by the function $g(\nu)$ defined as

$$g(\nu) = \frac{(n_0\nu^2 + \nu_e^2 / \pi^2)\nu_{pe}^2 \sin^2(\nu\tau_L 2\pi)}{(\nu^2 - \nu_{pe}^2)^2 + \nu_e^2\nu^2 (1 - (\nu\tau_L)^2)^2}, \quad (1)$$

where ν_{pe} is the plasma electronic frequency in Hz, ν_e is the electron collision frequency and $\tau_L=50$ fs is the laser pulse duration. We fit the measurements by convoluting the filters transmission to the distribution $g(\nu_{pe}, \nu_e)$. ν_{pe} determines the maximum of the distribution and ν_e its width. Since water vapour absorption is important in the spectral range > 1 THz, we include in the calculations a corresponding correction based on measurements of the water absorption spectrum made by Xin et al. ⁹, considering 40 % humidity and a path of 25 cm for the THz.

From the best fit of $g(\nu)$ we extract the percent of energy for each filter and the corresponding parameters ν_{pe} and ν_e . The values for the different F are reported in Table I. Knowing the plasma frequency ν_{pe} we can calculate the average plasma density inside the filament $N_e = (4\pi^2 m_e \epsilon_0 \nu_{pe}^2)/e^2$. The values obtained for N_e are in agreement with the measurements made by Théberge et al. ¹¹ by a longitudinal diffractometry technique, as shown in Figure 3. When the focal of the lens F is increased, the average plasma electronic density N_e decreases rapidly to reach an asymptotic value for plasma column lengths exceeding a few tens of cm, corresponding to a proper self-guided regime.

To estimate the conversion efficiency from laser to transition-Cherenkov THz emission, we compared it with the THz produced by Four Waves Mixing of the fundamental laser beam with its second harmonic in air. We reproduced the experiment of Cook et al. ⁷ with a 200 μ J, 50 fs IR pulse. According to ref. ¹² the energy of this THz pulse is ~ 0.1 nJ and its conversion efficiency defined as $\epsilon = W_{THz}/W_{laser}$ is 5×10^{-7} . From the relative measured signals we deduce the energy of the transition-Cherenkov emissions W_{THz} obtained with the different focal lengths (see table I). For filaments length exceeding 10 cm the conversion efficiency is found to be $\epsilon \sim 5 \times 10^{-10}$, which is in agreement with theoretical predictions³⁻⁴.

Finally, using the spectral distributions obtained from best fits with formula (1) and the energy calibration, we calculated the energy spectral density in the frequency range 0.1-3 THz for the different plasma filaments considered (see Figure 4). One can notice that the energy of the THz pulse is maximum for the 1000 mm lens and then decreases for longer filaments. This is partially explained by the decrease of the plasma electronic density N_e , and consequently, the decrease of plasma current directly responsible for THz emission. In addition, the collection of the THz is less efficient with our setup when the filament exceeds 10 cm, because a significant part of the emission passes through the hole of mirror M, since the emission cone angle is inversely proportional to the filament length³.

As a final remark, we note that the conversion efficiency of the transition-Cherenkov emission from filament is 1000 times smaller than the FWM method. However, considering the strong attenuation encountered by THz radiation in air under normal humidity conditions^{9,13}, it nevertheless surpasses in terms of effective irradiance other tabletop sources (FWM mixing, semiconductor antennas, optical rectification in crystals...^{5,12}) after only two meters of propagation. This illustrates the advantage of filaments for broadband THz illumination of remote targets.

The authors are grateful to B. Prade, C. D'Amico and V. Parmentier for their help and for fruitful discussions. We acknowledge partial support by DGA.

¹H. Hamster, A. Sullivan, S. Gordon, W. White and R.W. Falcone, Phys. Rev. Lett. **71** 2715 (1993).

²T. Bartel, P. Gaal, K. Reimann, M. Woerner and T. Elsaesser, Opt. Lett. **30**, 2805 (2005).

³C. D'Amico, A. Houard, M. Franco, B. Prade, A. Couairon, V.T. Tikhonchuk and A. Mysyrowicz, Phys. Rev. Lett. **98**, 235002 (2007).

⁴C. D'Amico, A. Houard, S. Akturk, Y. Liu, M. Franco, B. Prade, A. Mysyrowicz, A. Couairon, J. Le Bloas and V. T. Tikhonchuk, *submitted to New Journal of Physics* (2007).

⁵K. Reimann, Rep. Prog. Phys. **70**, 1597 (2007).

⁶Y. Liu, A. Houard, B. Prade, S. Akturk, A. Mysyrowicz and V.T. Tikhonchuk, Phys. Rev. Lett. **99**, 135002 (2007).

⁷D.J. Cook and R.M. Hochstrasser, Opt. Lett. **25**, 1210 (2000).

⁸G. Méchain, S. Tzortzakis, B. Prade, M. Franco, A. Mysyrowicz and B. Leriche, Appl. Phys. B **77**, 707 (2003).

⁹X. Xin, H. Altan, A. Saint, D. Matten and R. R. Alfano, Journal of Applied Physics **100**, 094905 (2006).

¹⁰A. Couairon and A. Mysyrowicz, Phys. Rep. **441**, 47 (2007).

¹¹F. Théberge, W. Liu, P.T. Simard, A. Becker and S.L. Chin, Phys. Rev. E **74**, 036406 (2006).

¹²T. Löffler, M. Kress, M. Thomson, T. Hahn, N. Hasegawa and H. G. Roskos, Semicond. Sci. Technol. **20**, S134 (2005).

¹³A.W.M. Lee, Q.Kumar, B.S. Williams, Q. Hu and J.L. Reno, Appl. Phys. Lett. **89**, 141125 (2006).

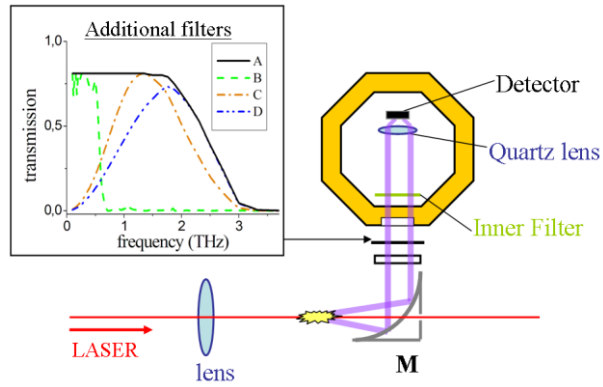


FIG 1. Experimental setup. Inset: spectral transmission of the additional filters B, C and D in the range 0 - 3.5 THz.

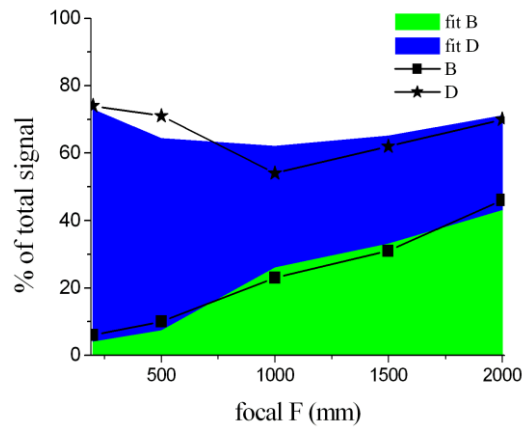


FIG 2. Ratio of energy measured with the different filters (in %) for different focal F: experimental measurements (dots) and theoretical fit (coloured areas).

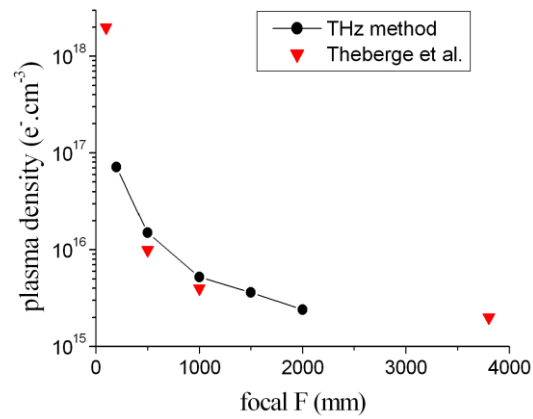


FIG 3. Plasma electronic density N_e extracted from the fit to equation (1) for different focal lengths F (dots). Also shown for comparison are the values measured in ref 6 (triangles).

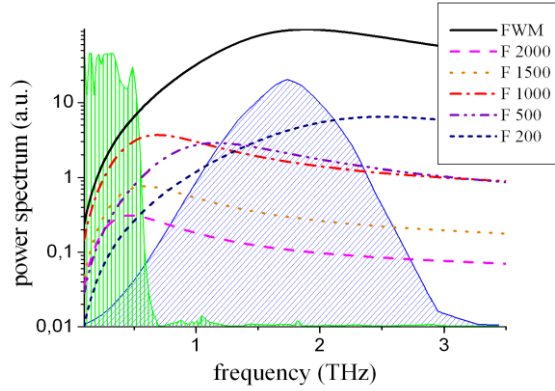


FIG 4. THz power spectrum extracted from the best fit to formula (1) for different focusing lenses F . The continuous line represents the fit for the Four Wave Mixing emission of a 200 μJ two-colour pulse. Also shown in dashed area are the transmission windows of the filters B and D (in arbitrary units).

TABLE I. The table presents for each value of the focal length F the estimated length L of the plasma filament, the total signal measured with the filter A, the ratio of this total signal measured with the filters B, C and D (experimental and best fit). From this fit we obtain the plasma frequency ν_{pe} , the corresponding plasma density N_e and the electron collision frequency ν_e . Finally the last column shows the estimated energy of the THz pulse W_{THz} .

F (mm)	L (cm)	A (mV)	B		C		D		ν_{pe} (THz)	N_e (cm^{-3})	ν_e (THz)	W_{THz} (pJ)
			exp.	fit (%)	exp.	fit (%)	exp.	fit (%)				
200	3	45	6	4	52	63	68	69	2.4	7.7×10^{16}	2.5	4.5
500	5	48.2	10	9.7	53	60	61	51	1.1	2.1×10^{16}	1.3	4.8
1000	10	75	23	26	39	45	31	36	0.65	5.2×10^{15}	0.9	7
1500	13	16	31	33	36	40	31	32	0.54	3.7×10^{15}	0.8	1.6
2000	25	6.7	46	43	31	35	24	28	0.44	3×10^{15}	0.7	0.7